Solvent effects on the photophysical and photochemical properties of (*E*,*E*,*E*)-1,6-bis(4-nitrophenyl)hexa-1,3,5-triene

Yoriko Sonoda,*†[a] Wai Ming Kwok,[a] Zdenék Petrasek,[a] Richard Ostler,[a] Pavel Matousek,[b] Michael Towrie,[b] Anthony W. Parker[b] and David Phillips[a]

[a] *Department of Chemistry, Imperial College of Science, Technology and Medicine, Exhibition Road, London, UK SW7 2AY*
[b] *Central Laser Facility, Rutherford Appleton Laboratory, Chilton, Didcot, Oxfordshire, UK OX11 0QX*

Received (in Cambridge, UK) 30th October 2000, Accepted 17th January 2001
First published as an Advance Article on the web 16th February 2001

The photophysical and photochemical properties of (*E*,*E*,*E*)-1,6-bis(4-nitrophenyl)hexa-1,3,5-triene [(*E*,*E*,*E*)-**1**] have been studied in various solvents. The fluorescence emission maxima of (*E*,*E*,*E*)-**1** show an increasing Stokes shift with increasing solvent polarity. Picosecond time-resolved fluorescence (TF) and transient absorption (TA) spectra do not show any significant time-dependent shifts in nonpolar solvent whereas, in more polar solvents, large red and blue shifts are observed in the TF and TA spectra, respectively. The fluorescence quantum yield reaches a maximum in moderately polar solvents and the quantum yield of intersystem crossing decreases strongly with increasing solvent polarity. *Z*–*E*-Isomerization of triene double bonds is inefficient in all solvents. In contrast, the absorption and fluorescence maxima for (*E*,*E*,*E*)-1,6-bis(4-cyanophenyl)hexa-1,3,5-triene [(*E*,*E*,*E*)-**2**] are practically solvent-independent. When the solvent polarity is increased, fluorescence quantum yield decreases monotonically and *Z*–*E*-isomerization quantum yield increases strongly. The results for (*E*,*E*,*E*)-**1** can be understood in terms of an additional charge transfer excited state, which is absent for (*E*,*E*,*E*)-**2**.

Introduction

α,ω-Diphenylpolyenes have been extensively studied because they are model compounds for biological structures such as vitamin A, carotenoids and visual pigments. Among these polyenes (*E*,*E*,*E*)-1,6-diphenylhexa-1,3,5-triene [(*E*,*E*,*E*)-DPH] has attracted much attention, mainly because of its unique fluorescence behavior. DPH is known to exhibit dual fluorescence originating from $S_1(A_g)$ and $S_2(B_u)$ at thermal equilibrium.[1,2] In addition to the spectroscopic studies, photochemical properties such as *Z*–*E*-isomerization of DPH have attracted considerable attention[3] and it has been shown that the introduction of substituents on to the phenyl group affects the isomerization strongly.[4] For biological applications, DPH and its derivatives are widely used for fluorescence probes in membrane studies because of their fluorescence anisotropy.[5] The electron push–pull type of DPH has been shown to be potentially useful in nonlinear optics due to the giant dipole moment induced by substituents.[6]

Aromatic nitro compounds are normally nonfluorescent or weakly fluorescent, since singlet–triplet intersystem crossing, predissociation of nitro groups, hydrogen abstraction and addition to double bonds are efficient deactivation pathways from n–π* excited states.[7] However, the dinitro-substituted DPH [(*E*,*E*,*E*)-**1**] is exceptionally fluorescent and it has been shown that the fluorescence spectrum of (*E*,*E*,*E*)-**1** shifts to longer wavelengths as the solvent polarity is increased.[8] A similar solvent-dependent red-shift is also observed for mononitro-substituted DPH.[8,9] For (*E*,*E*,*E*)-**1**, it is suggested that the formation of an (intramolecular) charge transfer excited state in polar solvents results in the red-shifted fluorescence emission.[8] In earlier studies, however, only steady-state fluorescence properties were investigated and the structure of the charge transfer state is not clear. Measurements of transient spectra would provide important insight into the charge transfer state. It is also necessary to determine the quantum yields of intersystem crossing and *Z*–*E*-isomerization to fully understand the photophysical and photochemical behavior of (*E*,*E*,*E*)-**1**.

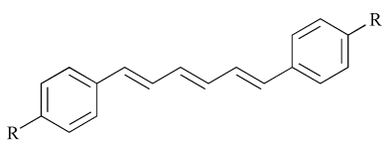

(*E*,*E*,*E*)-**1**: R = NO_2
(*E*,*E*,*E*)-**2**: R = CN

In this study, picosecond time-resolved fluorescence (TF) and transient absorption (TA) spectra, in addition to steady-state absorption and fluorescence spectra, were measured for (*E*,*E*,*E*)-**1** in various solvents with different polarities. Fluorescence lifetimes (τ_s) and quantum yields of fluorescence (φ_{flu}), intersystem crossing (φ_{isc}) and *Z*–*E*-isomerization were also measured. Spectroscopic studies were also conducted for the dicyano-substituted DPH [(*E*,*E*,*E*)-**2**]. For (*E*,*E*,*E*)-**2**, only absorption and fluorescence data in hexane and chloroform solvents are known.[8a] In spite of having electron-withdrawing groups of similar strength, the photophysical and photochemical properties of (*E*,*E*,*E*)-**1** and (*E*,*E*,*E*)-**2** differed entirely.

Experimental

General procedures

Absorption spectra were recorded on Hewlett Packard HP 8453 and Perkin-Elmer UV/vis Lambda 2 spectrometers. Corrected fluorescence spectra were recorded using a Spex FluoroMax spectrometer. ^{1}H NMR spectra were recorded on a Varian Gemini-300 BB spectrometer (300 MHz) in $CDCl_3$ with $SiMe_4$ as internal standard. *J* values are given in Hz. Isomerization

† Present address: National Institute of Materials and Chemical Research, 1-1 Higashi, Tsukuba, Ibaraki 305-8565, Japan.

 DOI: 10.1039/b008711o

Table 1 Absorption and fluorescence maxima and Stokes shifts for (*E*,*E*,*E*)-**1** and (*E*,*E*,*E*)-**2**

Solvent	$E_T(30)$/ kcal mol^{-1} [a]	(*E*,*E*,*E*)-**1**			(*E*,*E*,*E*)-**2**		
		λ_{abs}/nm	λ_{em}/nm	ΔE_{ss}/cm^{-1}	λ_{abs}/nm	λ_{em}/nm	ΔE_{ss}/cm^{-1}
MCH	31.2[b]	395	460	3577	374	450	4516
Carbon tetrachloride	32.5	402	472	3690	378	452	4331
Toluene	33.9	410	491	4023	380	452	4192
Dioxane	36.0	408	493	4226	378	452	4331
Tetrahydrofuran	37.4	411	508	4646	379	452	4261
Chloroform	39.1	414	542	5705	380	451	4143
Dichloromethane	41.1	415	549	5864	379	452	4261
Acetone	42.2	411	554	6280	375	452	4543
Dimethylformamide	43.8	422	578	6396	382	455	4200
AN	46.0	410	580	7149	375	452	4543

[a] Taken from ref. 19. [b] The value for cyclohexane.

photoproducts were analyzed by TOSOH CCPD/SD-8013/SC-8020 HPLC monitored by a Photal MCPD 3600 multichannel photodetector. A Merck LiChroCART 250-4 column filled with LiChrosorb Si 60 (5 μm) was used.

Values of φ_{flu} were determined using a solution of quinine sulfate in sulfuric acid (0.5 M) as a standard ($\varphi_{flu} = 0.546$).[10] Values of τ_s were measured by the time-correlated single-photon counting (TCSPC) method. The excitation wavelength was 400 nm for (*E*,*E*,*E*)-**1** and 375 nm for (*E*,*E*,*E*)-**2** unless otherwise noted. Diluted solutions ($< 1.5 \times 10^{-6}$ M, < 0.1 OD at the excitation wavelength), degassed by freeze–thaw cycles, were used for all fluorescence measurements.

TF and TA spectra were measured at the Lasers for Science Facility, Rutherford Appleton Laboratory (RAL), UK. Sample solutions were excited with 400 nm light obtained by frequency doubling of 800 nm output from a titanium-sapphire laser[11] and TF spectra were obtained using an optical Kerr gate.[12] Time resolutions of TA and TF measurements were around 600 fs and 2–3 ps, respectively. The concentration of the samples was 6×10^{-6} M in methylcyclohexane (MCH), 4×10^{-5} M in toluene, 3×10^{-4} M in chloroform and 1×10^{-4} M in acetonitrile (AN); the samples were not degassed. For the transient measurements, flowing samples were used to avoid the decomposition of the samples during laser excitation.

Triplet–triplet (T–T) molar absorption coefficients were determined by comparing triplet and ground state absorptions in T–T spectra, according to the method described in the literature.[13] Values of φ_{isc} were determined using the comparative method.[13,14] A solution of zinc tetraphenylporphine in toluene was used as a standard [ε_T/dm^3 mol^{-1} cm^{-1} = 71 000 (470 nm) and $\varphi_{isc} = 0.88$].[15,16] Triplet lifetimes (τ_T) were determined from the decay curves of T–T absorption. For the triplet measurements a nitrogen-dye laser system was used to excite the samples. The excitation wavelength was 400 nm. All sample solutions were diluted (3×10^{-6} M in MCH and 1.5×10^{-5} M in toluene, chloroform and AN) and degassed by freeze–thaw cycles.

Quantum yields of *Z*–*E*-isomerization were determined using a solution of (*E*,*E*,*E*)-1,6-bis(4-formylphenyl)hexa-1,3,5-triene in AN as a standard (*E*,*E*,*E*→*Z*,*E*,*E* isomerization quantum yield $\varphi_{EEE\text{-}ZEE} = 0.325$).[4b] The *Z*,*E*,*E*-isomer was identified from ^{1}H NMR and UV/vis spectroscopy. Isomer ratios of photostationary states were determined by HPLC analysis. The excitation wavelength region was 411 ± 7 nm. A 2 KW spectro-irradiator was used as a light source, the sample concentration was 2.5×10^{-5} M. For the isomerization measurements, solutions were degassed by argon bubbling.

Materials

All solvents for preparing solutions were of UV spectroscopic grade (Aldrich) and used without further purification.

(*E*,*E*,*E*)-**1** and (*E*,*E*,*E*)-**2** were prepared by Wittig reactions of 4-nitrobenzaldehyde and 4-cyanobenzaldehyde, respectively, with (*E*)-1,4-bis[chloro(triphenyl)phosphoranyl]but-2-ene according to the modified method described in the literature.[17]

(*E*,*E*,*E*)-1,6-Bis(4-nitrophenyl)hexa-1,3,5-triene [(*E*,*E*,*E*)-1]. Mp 201–202 °C (from toluene) (lit.,[8b] 195–197 °C); δ_H ($CDCl_3$) 8.20 (4H, d, *J* 8.9, arom), 7.55 (4H, d, *J* 8.9, arom), 7.05 (2H, ddd, *J* 15.7, 7.2 and 3.0, triene 2-H and 5-H), 6.71 (2H, d, *J* 15.4, triene 1-H and 6-H), 6.66 (2H, dd, *J* 7.4 and 2.7, triene 3-H and 4-H); UV/vis (AN) λ_{max}/nm 410 (ε/dm^3 mol^{-1} cm^{-1} 76 400).

(*E*,*E*,*E*)-1,6-Bis(4-cyanophenyl)hexa-1,3,5-triene [(*E*,*E*,*E*)-2]. Mp 223–224 °C (from toluene) (lit.,[18] 210–212 °C); δ_H ($CDCl_3$) 7.61 (4H, d, *J* 8.5, arom), 7.49 (4H, d, *J* 8.3, arom), 6.99 (2H, ddd, *J* 15.5, 7.1 and 3.0, triene 2-H and 5-H), 6.64 (2H, d, *J* 15.3, triene 1-H and 6-H), 6.60 (2H, dd, *J* 6.8 and 3.2, triene 3-H and 4-H); UV/vis (AN) λ_{max}/nm 375 (ε/dm^3 mol^{-1} cm^{-1} 66 000).

Results

Steady-state absorption and fluorescence spectra

Absorption and fluorescence maxima (λ_{abs} and λ_{em}, respectively), and Stokes shifts ($\Delta E_{ss} = \bar{\nu}_{abs} - \bar{\nu}_{em}$) for (*E*,*E*,*E*)-**1** and (*E*,*E*,*E*)-**2** in various solvents are summarized in Table 1. As a measure of the solvent polarity, the Dimroth parameter ($E_T(30)$)[19] was used.

Absorption spectra. Figs. 1 and 2 show absorption spectra of (*E*,*E*,*E*)-**1** and (*E*,*E*,*E*)-**2**, respectively. Values of λ_{abs} for (*E*,*E*,*E*)-**1**, where available, were in good agreement with those reported in the literature.[8b]

Absorption spectra of (*E*,*E*,*E*)-**1** showed a small, but significant, solvent dependence moving to longer wavelengths with increasing solvent polarity. In nonpolar MCH the spectra had distinct vibrational structure with spacings of 1393 and 1209 cm^{-1}, corresponding to the C=C and C–C stretches of conjugated polyenes.[2] As the polarity was increased, the profile became broad and structureless, suggesting large solute–solvent interactions in polar solvents.

In contrast, absorption spectra of (*E*,*E*,*E*)-**2** did not show any significant solvent-dependent shifts and vibrational structure was observed even in AN. Further, the structure observed in MCH was more distinct for (*E*,*E*,*E*)-**2** than for (*E*,*E*,*E*)-**1** (Figs. 1(a) and 2(a)), due to smaller solute–solvent interaction in (*E*,*E*,*E*)-**2**.

Fluorescence spectra. Figs. 1 and 2 show steady-state fluorescence spectra of (*E*,*E*,*E*)-**1** and (*E*,*E*,*E*)-**2**, respectively. Values of λ_{em} for (*E*,*E*,*E*)-**1** in nonpolar and low polarity solvents (such as MCH and toluene) were in good agreement with those in the

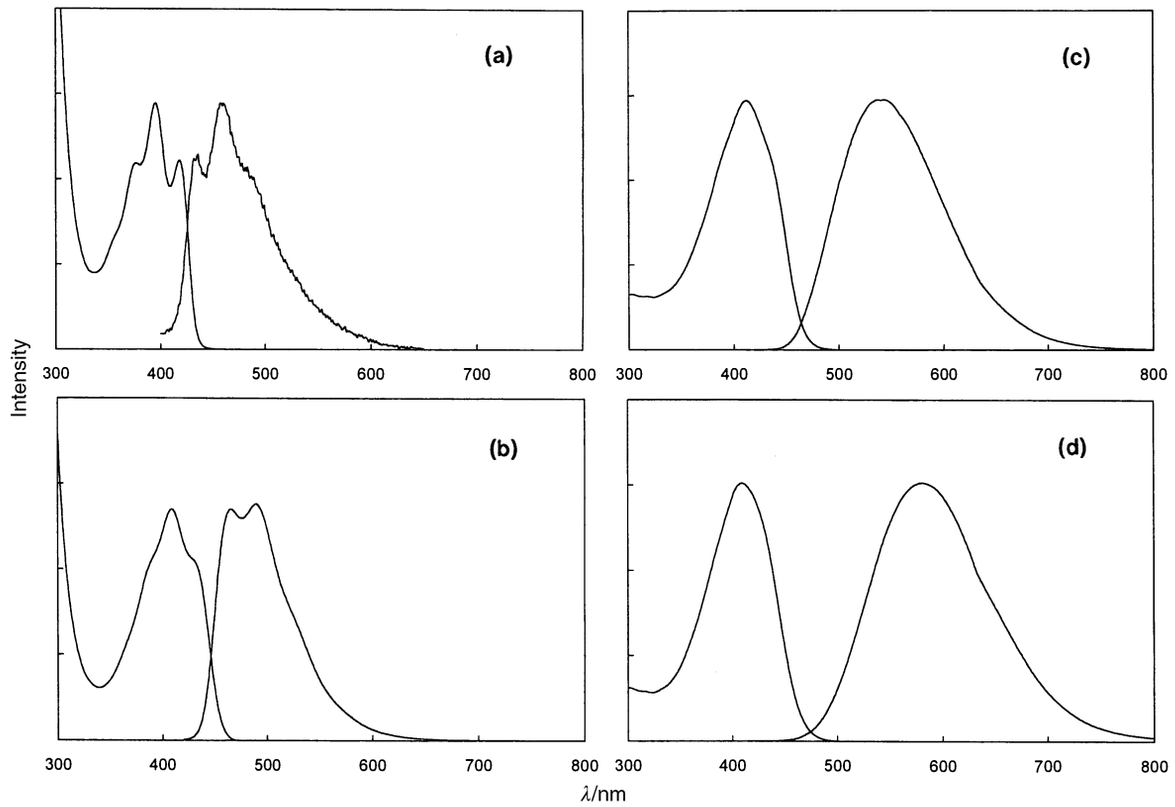

Fig. 1 Absorption and fluorescence spectra of (*E*,*E*,*E*)-**1** in (a) MCH (excitation wavelength = 350 nm), (b) toluene, (c) chloroform and (d) AN.

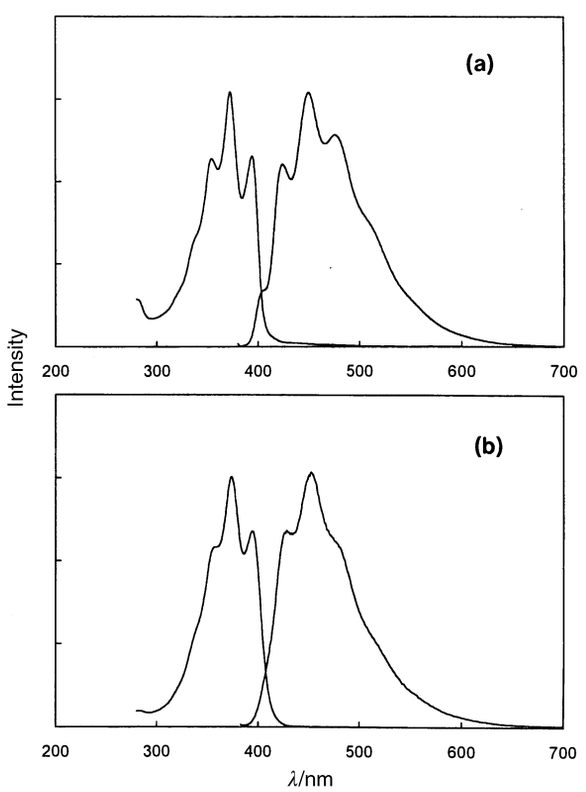

Fig. 2 Absorption and fluorescence spectra of (*E*,*E*,*E*)-**2** in (a) MCH and (b) AN.

literature.[8] However, the observed λ_{em} in moderately and highly polar solvents (such as chloroform and AN) were somewhat shorter than the reported values. This is possibly due to the extremely high sensitivity of the fluorescence spectra of (*E*,*E*,*E*)-**1** to the environment (for example, to temperature) since there is also a discrepancy between the data in refs. 8(*a*) and 8(*b*). For (*E*,*E*,*E*)-DPH, the ground-state concentration of s-*Z* conformers increases at higher temperature, leading to enhanced emission in the longer wavelength region of the fluorescence spectrum.[20] Similarly, its conformational flexibility in the ground state may contribute to influence the emission properties of (*E*,*E*,*E*)-**1**.

As reported earlier,[8b] fluorescence spectra of (*E*,*E*,*E*)-**1** were highly solvent-dependent and values of λ_{em} shifted to longer wavelengths as the solvent polarity increased. Since the spectrum in AN showed no concentration dependence, the red-shift is not attributed to aggregation or complexation of the solute and solvent in the ground state. The spectrum in MCH showed distinct vibrational structure with spacings of 1358 and 1271 cm^{-1}. The mirror image relationship between absorption and fluorescence spectra was observed but, as the solvent polarity was increased, the structure disappeared to give a broad spectrum in AN.

The solvent-dependence of the fluorescence spectra for (*E*,*E*,*E*)-**2** was entirely different from that for (*E*,*E*,*E*)-**1**. Values of λ_{em} for (*E*,*E*,*E*)-**2** were practically solvent-independent. The shapes of the spectra, on the other hand, changed significantly. In MCH the spectrum showed vibrational structure, but was not a close mirror image of the absorption spectrum. However, when the solvent polarity was increased, the spectrum became less structured and reverted almost to the mirror image of the absorption.

Stokes shifts. When $E_T(30)$ was increased, ΔE_{ss} for (*E*,*E*,*E*)-**1** increased almost linearly, whereas that for (*E*,*E*,*E*)-**2** showed no fundamental change. The solvent dependence of ΔE_{ss} for (*E*,*E*,*E*)-**2** is similar to that for (*E*,*E*,*E*)-DPH.[9]

Fluorescence quantum yields

Table 2 gives φ_{flu} for (*E*,*E*,*E*)-**1** and (*E*,*E*,*E*)-**2** in various solvents. The value of φ_{flu} for (*E*,*E*,*E*)-**1** in MCH was very small, rising with increasing solvent polarity to reach a maximum value in dichloromethane, before falling again as the solvent

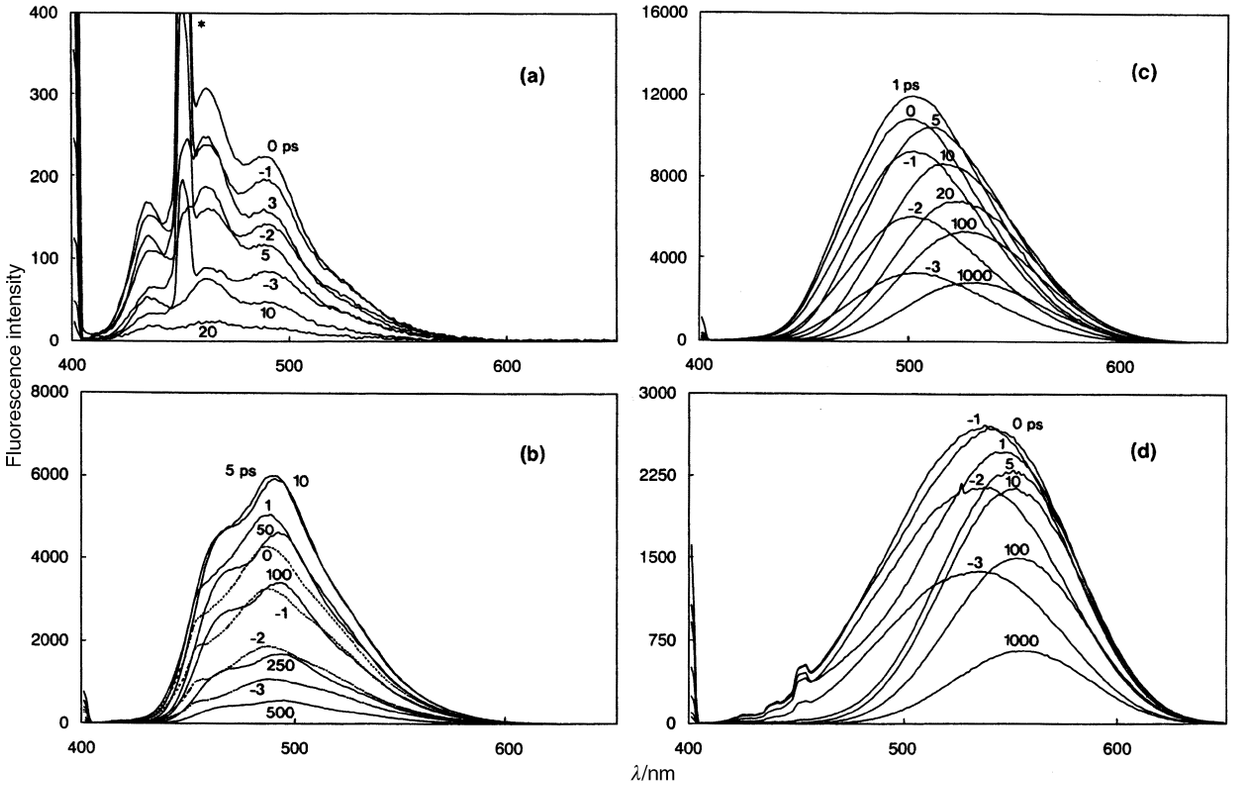

Fig. 3 Time-resolved fluorescence spectra of (*E*,*E*,*E*)-**1** in (a) MCH, (b) toluene, (c) chloroform and (d) AN. * Raman peak of the solvent.

Table 2 Fluorescence quantum yields[a] for (*E*,*E*,*E*)-**1** and (*E*,*E*,*E*)-**2**

Solvent	(*E*,*E*,*E*)-**1**	(*E*,*E*,*E*)-**2**
MCH	0.002	0.80
Carbon tetrachloride	0.015	
Toluene	0.10	0.88
Dioxane	0.28	
Tetrahydrofuran	0.53	
Chloroform	0.60	0.64
Dichloromethane	0.61	
Acetone	0.56	
Dimethylformamide	0.44	
AN	0.30	0.032

[a] ± 10%.

polarity was increased further. In contrast, φ_{flu} for (*E*,*E*,*E*)-**2** were large for MCH and toluene and, as for (*E*,*E*,*E*)-DPH,[9] φ_{flu} decreased dramatically with increasing solvent polarity.

Fluorescence lifetimes

Values of τ_s for (*E*,*E*,*E*)-**1** were measured in MCH, toluene, chloroform and AN. In MCH, τ_s was shorter than the time resolution (50–100 ps) of our single-photon counting apparatus. It was estimated to be < 5 ps from TF spectra and 4 ps from TA spectra (see below). In chloroform, mono-exponential fitting gave $\tau_s = 1.9$ ns ($\chi^2 = 10.9$) whereas bi-exponential fitting gave a better fit with $\tau_s = 2.0$ ns (36%) and $\tau_s = 0.05$ ns (64%) ($\chi^2 = 1.5$) using a monitoring wavelength $\lambda_{mon} = 460$ nm. Values of $\tau_s = 0.26$ ns and 0.1 ns were obtained for the fluorescence in toluene at $\lambda_{mon} = 440$ nm. In these solvents, the shorter decay component had a larger weight at shorter λ_{mon}. The decay in AN could be fitted by a mono-exponential function to give $\tau_s = 2.2$ ns at $\lambda_{mon} = 480$, 580 and 730 nm.

Time-resolved fluorescence and transient absorption spectra

Time-resolved fluorescence spectra. Fig. 3 shows the TF spectra of (*E*,*E*,*E*)-**1**. In MCH the spectra showed the same structure as the steady-state and did not show any time-dependent shifts. However, in toluene, chloroform and AN, the spectra became broader and less structured and all shifted to longer wavelengths on a few ps time-scale. The red-shift in toluene was small and fast with the peaks at 455 and 488 nm shifted to 468 and 493 nm within 5–10 ps after laser excitation. By contrast, the shift observed in chloroform was large and relatively slow. The shift time was ~ 20 ps. In AN the large shift was completed within 5 ps.

The TF spectra show that the fast lifetime components measured by TCSPC are limited by instrument response. For example, the TF measurements in chloroform give $\tau_s < 10$ ps at 460 nm, which is shorter than $\tau_s = 0.05$ ns determined from TCSPC, and the decay of TF, in AN, at 460 nm is clearly not mono-exponential at 2.2 ns but has a very fast (and large) component of ~ ps duration not resolved by TCSPC. It should also be noted that fluorescence intensities for wavelengths longer than 500 nm were reduced from the true spectra by optical filters and that the decay rates measured by TF are systematically lower than those measured by TCSPC due to changes in the alignment of the excitation beam as a function of delay line position. More quantitative work is now in progress to correct the spectra. However, the spectral features reported above remain valid.

Transient absorption spectra. The TA spectra of (*E*,*E*,*E*)-**1** were measured in MCH, toluene, chloroform and AN. All spectra of the initially-formed states are broad and structureless. In MCH λ_{abs} was found at 710 nm. It did not show any significant shifts with time, which corresponds to the observation in the TF spectrum. In toluene, chloroform and AN, the TA spectra shifted to shorter wavelengths on a ps time-scale. The spectrum in toluene showed a small blue-shift from 707 to 705 nm within 5–10 ps. The largest shift, from 700 to 686 nm, was observed in chloroform. It was completed within 20 ps. In AN, the peak at 666 nm shifted to 654 nm within 5 ps. Therefore, in contrast to the small solvent dependence of the steady-state absorption spectra, the TA spectra shifted to shorter wavelengths as the solvent polarity increased. This is

Table 3 T–T absorption maxima, molar absorption coefficients, triplet lifetimes and intersystem crossing quantum yields of (*E*,*E*,*E*)-**1**

Solvent	λ_T/nm [a]	ε_T/dm^3 mol^{-1} cm^{-1} [b]	τ_T/μs [c]	φ_{isc} [d]
MCH	517	1.2×10^5	60	0.89
Toluene	546	1.3×10^5	75	0.31
Chloroform	545	1.4×10^5	65	0.04
AN	552	1.9×10^5	80	<0.01

[a] ±2 nm. [b] ±15%. [c] ±10%. [d] ±15%.

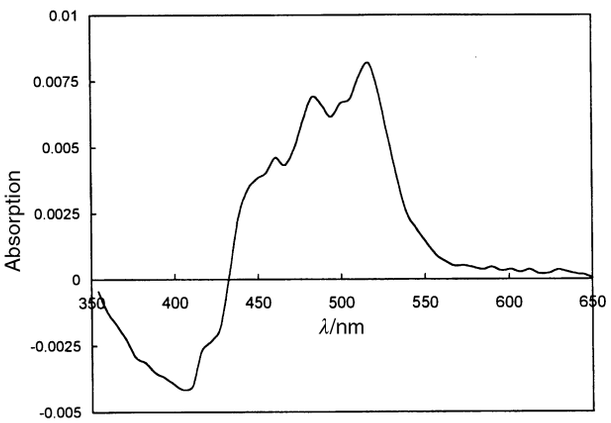

Fig. 4 T–T absorption spectrum of (*E*,*E*,*E*)-**1** in MCH.

consistent with the time-dependent red-shifts observed in the TF spectra.

Triplet–triplet absorption spectra, triplet lifetimes and quantum yields of singlet–triplet intersystem crossing

Values of T–T absorption maximum (λ_T), ε_T, τ_T and φ_{isc} of (*E*,*E*,*E*)-**1** are summarized in Table 3. Fig. 4 shows the T–T absorption spectrum (positive region; 430–570 nm) of (*E*,*E*,*E*)-**1** in MCH. The negative spectral region (350–430 nm) is due to the depletion of the electronic ground state, S_0. T–T absorption spectra were also obtained for solutions in toluene, chloroform and AN.

The T–T absorptions shifted to longer wavelengths as the solvent polarity was increased. The values of ε_T were similar to those for (*E*,*E*,*E*)-DPH.[13] The solvent dependence of τ_T was shown to be small. The value of φ_{isc} decreased dramatically with increasing solvent polarity.

Quantum yields of *Z*–*E*-isomerization

Irradiation of (*E*,*E*,*E*)-**1** in MCH or toluene gave no change in the UV/vis spectra, indicating that *E*→*Z* isomerization of (*E*,*E*,*E*)-**1** is inefficient in these solvents. In AN, *E*,*E*,*E*→*Z*,*E*,*E* isomerization was observed. Irradiation in AN with 411 ± 7 nm light gave a photostationary mixture of *E*,*E*,*E* and *Z*,*E*,*E* isomers in the ratio of 92 : 8. However, the quantum yield of the isomerization was very low ($\varphi_{EEE-ZEE} = 0.002$).

The solvent dependence of the isomerization quantum yield for (*E*,*E*,*E*)-**2** was in strong contrast to that for (*E*,*E*,*E*)-**1**. Although *E*→*Z* isomerization was inefficient in MCH and toluene, (*E*,*E*,*E*)-**2** underwent efficient *E*,*E*,*E*→*Z*,*E*,*E* isomerization in AN ($\varphi_{EEE-ZEE} = 0.46$).[4c] The isomer ratio was *E*,*E*,*E* : *Z*,*E*,*E* = 37 : 63 for the photostationary state reached by irradiation with 374 ± 7 nm light.[4c] A similar solvent dependence of the isomerization quantum yield is commonly observed for ring-substituted derivatives of DPH.[4c]

Discussion

Steady-state absorption and fluorescence spectra

(*E*,*E*,*E*)-DPH is known to exhibit dual fluorescence from two different excited states, covalent $S_1(A_g)$ and ionic $S_2(B_u)$, which are at thermal equilibrium.[1,2] Since the absorption is due to the allowed $S_0(A_g)$–$S_2(B_u)$ transition, the mirror image relationship between absorption and fluorescence spectra is not observed. For (*E*,*E*,*E*)-**1**, on the other hand, the mirror image relationship was observed in MCH and this has been attributed to enhanced fluorescence emission from S_2,[8b] even in nonpolar solvents. The introduction of polar substituents, such as NO_2 groups, to the phenyl rings of DPH acts to stabilize the ionic S_2 selectively, leading to a decrease in the energy gap (ΔE_{12}) between S_1 and S_2[21] and, in turn, to more effective S_1–S_2 mixing, which increases the relative fluorescence intensity from S_2.[22,23]

Contrary to this, the fluorescence spectrum of (*E*,*E*,*E*)-**2** in MCH did not show a close mirror image relationship with the absorption spectrum. This is similar to the case of (*E*,*E*,*E*)-DPH, suggesting that (*E*,*E*,*E*)-**2** displays dual fluorescence from S_1 and S_2. This implies that, although (*E*,*E*,*E*)-**2** has a polar substituent, CN, ΔE_{12} is still large in nonpolar solvents, such as MCH. In more polar solvents, ΔE_{12} decreases, enhancing the intensity of the fluorescence from S_2, thus making the fluorescence spectrum become closer to the mirror image of the absorption spectrum.

The small ΔE_{ss} and the mirror image relationship observed for (*E*,*E*,*E*)-**1** in MCH show that the excited state for the fluorescence is the same as that for the absorption. This state on the S_2 surface is produced from planar S_0 by the Franck–Condon transition. Therefore, it probably has a near-planar conformation, in which the π-orbitals of the triene and phenyl groups are almost parallel with respect to the NO_2 group. Although charge transfer may occur partially from the electron-donating triene-phenyl π-system to the electron-withdrawing NO_2 group, there are some mesomeric interactions between them. The large ΔE_{ss} observed in AN shows that the excited state responsible for the fluorescence emission is different from that for the absorption. This state seems to be an intramolecular (or a 1 : 1 solvent–solute complex) charge transfer state (CT*), which has a larger dipole moment than the near-planar state (*EEE**), since it is more apparent in polar solvents. The broad and structureless fluorescence spectrum in AN suggests that the emission from CT* occurs to a repulsive potential. For the CT* state the π-orbitals of the triene and phenyl groups are probably orthogonal with respect to the NO_2 group, leading to a break in the conjugation.[24] The resulting decoupled π-orbital conformation leads to the full charge transfer from the triene-phenyl to the NO_2 groups. Most probably, the twisting occurs at the single bond between the NO_2 and phenyl groups but, in alternative structures, the single bond between the phenyl and double bonds or two double bonds might be twisted. In nonpolar solvents, the charge transfer (CT) process from *EEE** or CT* is inefficient, and in this case fluorescence emission mainly occurs from *EEE**. In moderately polar solvents, the CT process becomes more efficient and is expected to lead to dual fluorescence from both states. In polar solvents, the CT process is highly efficient and fluorescence from the CT* state is mainly observed in this case.

In contrast, the solvent-independent small ΔE_{ss} for (*E*,*E*,*E*)-**2** shows that the fluorescence is mostly derived from the same excited state that is responsible for the absorption. Since the solvent dependence of the absorption and fluorescence spectra are small, the dipole moment of this state is considered to be small.

Although the NO_2 and CN electron-withdrawing groups have similar strength (Hammett parameter $\sigma_p = 0.78$ and 0.66 for NO_2 and CN, respectively),[25] no CT process seems to occur for (*E*,*E*,*E*)-**2**. This can be understood in terms of the intrinsic nature of the CN triple bond. The twisting of the CN–phenyl single bond does not lead to a break in conjugation between the CN and phenyl groups, resulting to the low degree of charge transfer of the excited state.

Fluorescence lifetimes

Although the shorter decay component could not be determined accurately due to experimental limits, bi-exponential decay behavior was suggested for (*E*,*E*,*E*)-**1** in toluene and chloroform. This strongly supports the idea of the dual fluorescence from *EEE** and CT* in moderately polar solvents. The shorter decay component should correspond to the fluorescence from *EEE**, since it has a larger weight at shorter λ_{mon}. In AN, the 2.2 ns decay probably corresponds to pure CT* fluorescence. The value of τ_s for the *EEE** fluorescence in AN could not be obtained by the present decay measurements, due to the very fast CT process in polar solvents.

Time-resolved fluorescence and transient absorption spectra

No time-dependent shift was observed in the TF or TA spectrum of (*E*,*E*,*E*)-**1** in MCH. This is consistent with the assumption that only the *EEE** state is responsible for the fluorescence emission in nonpolar solvents. The large red-shifts in the TF and the blue-shifts in the TA spectra observed in toluene, chloroform and AN can be understood as a result of the CT process. The stabilization of CT* relative to *EEE** leads to a smaller CT*–S_0 energy gap than *EEE**–S_0, and therefore, a larger CT*–S_n gap than *EEE**–S_n. Since the TF spectra in these solvents did not show any significant changes from −3 to −1 ps delay time, the spectra at −3 ps are considered to be the emission from the pure *EEE** state. The spectra at 500 ps to 1 ns are probably due to the emission from pure CT*, because the lifetimes for the *EEE** emission are very short (< 0.1 ns).

The observed time-dependent shifts in the TF spectra are attributed to the stabilization of CT* relative to *EEE** resulting from the geometry change (twisting motion) of the solute which accompanies the CT process, and the stabilization of the CT* by solvent reorganization.[24] If we assume that the overall rate of the shifts is governed by the rate of the geometry change, the slow shifts in chloroform can be explained by a slow geometry change resulting from an energy barrier along the pathway from *EEE** to CT*. In AN the geometry change is expected to be faster than that in chloroform due to the absence of the barrier.

Photophysical and photochemical processes

(*E*,*E*,*E*)-**1** showed a maximum φ_{flu} in moderately polar solvents. Since no similar solvent effect on φ_{flu} was observed for (*E*,*E*,*E*)-**2**, the dependence for (*E*,*E*,*E*)-**1** should be due to the presence of an additional non-radiative decay channel connected with the NO_2 group. The very small value of φ_{flu} in nonpolar solvents must correspond to an efficient singlet–triplet intersystem crossing, considering the large value of φ_{isc} ($\varphi_{flu} = 0.002$ and $\varphi_{isc} = 0.89$ in MCH). The large value of φ_{isc} can be attributed to the n–π* character of the excited state due to the NO_2 group, which is commonly observed for aromatic nitro compounds[7] such as 4,4′-dinitrostilbene ($\varphi_{isc} = 0.81$ in benzene).[26] Dinitrostilbene is known to undergo efficient *Z*–*E*-isomerization *via* triplet states in nonpolar (and polar) solvents.[27] In contrast, (*E*,*E*,*E*)-**1** showed no isomerization in MCH. This is tentatively explained in terms of the equilibrium between the near-planar and double-bond twisted triplet states. The minimum on the triplet energy potential surface for (*E*,*E*,*E*)-**1** possibly occurs at a twisting angle of less than 90°. As the solvent polarity is increased, the CT process becomes more efficient, leading to the increase in the intensity of the CT* fluorescence. The value of φ_{flu} increased and, accordingly, φ_{isc} decreased ($\varphi_{flu} = 0.10$ and $\varphi_{isc} = 0.31$ in toluene). When the solvent polarity is increased further, the efficiency of the CT process increased, resulting in strong dual fluorescence from *EEE** and CT*. For example, the total φ_{flu} reached a maximum ($\varphi_{flu} = 0.61$ in dichloromethane) and, accordingly, φ_{isc} decreased ($\varphi_{isc} = 0.04$ in chloroform). In highly polar solvents, the CT process is very efficient, and fluorescence emission occurs mainly from CT*. However, the value of φ_{flu} significantly decreased ($\varphi_{flu} = 0.30$ in AN) when compared to values in moderately polar solvents. Since the values of φ_{isc} and $\varphi_{EEE\text{–}ZEE}$ were small ($\varphi_{isc} < 0.01$ and $\varphi_{EEE\text{–}ZEE} = 0.002$ in AN), the nonradiative deactivation process from CT* which corresponds to the decrease in φ_{flu} must be an internal conversion to S_0. The increased efficiency of internal conversion can be attributed to the large stabilization of CT* by strong solute–solvent interaction, which leads to the decrease in the CT*–S_0 energy gap.

For (*E*,*E*,*E*)-**2**, on the other hand, φ_{flu} decreased monotonically as the polarity of the solvent increased. In nonpolar solvents, the singlet excited state deactivates mainly by fluorescence emission ($\varphi_{flu} = 0.80$ in MCH). As the solvent polarity increased, φ_{flu} decreased and $\varphi_{EEE\text{–}ZEE}$ increased strongly ($\varphi_{flu} = 0.032$ and $\varphi_{EEE\text{–}ZEE} = 0.46$ in AN). Thus in highly polar solvents, fluorescence emission is no longer an important deactivation pathway and *Z*–*E*-isomerization becomes more efficient. If we assume, by analogy with stilbene,[1] *E*,*E*,*E*→*Z*,*E*,*E* isomerization *via* the twisted excited state *pEE** and 1 : 1 partitioning from the *pEE** to the *E*,*E*,*E* and *Z*,*E*,*E* isomers, the efficiency of *EEE**→*pEE** conversion reaches a value as high as 0.92.

Conclusion

(*E*,*E*,*E*)-**1** shows highly solvent-dependent photophysical and photochemical behavior, which can be explained by the assumption of two different excited states, a low-polarity *EEE** state and a highly polar CT* state. Solvent dependence of the photophysical and photochemical processes for (*E*,*E*,*E*)-**2** is more similar to that for (*E*,*E*,*E*)-DPH than (*E*,*E*,*E*)-**1**, probably due to the absence of a CT* state for (*E*,*E*,*E*)-**2**. For (*E*,*E*,*E*)-**1**, the twisting of the single bond between the phenyl and NO_2 groups breaks the conjugation of the phenyl-triene π-system with NO_2 to lead the full charge transfer from the π-system to NO_2, whereas for (*E*,*E*,*E*)-**2** the conjugation between CN and the phenyl-triene system reduces the degree of charge transfer of the excited state. Quantum yield measurements show that (*E*,*E*,*E*)-**1** has a nonradiative relaxation pathway from the CT* state which does not involve *Z*–*E*-isomerization.

Acknowledgements

We thank Dr C. Ma and Dr S. Murata for valuable discussions. The Japan Industrial Technology Association (JITA) is gratefully acknowledged for the support of a fellowship.

References

1 M. T. Allen and D. G. Whitten, *Chem. Rev.*, 1989, **89**, 1691.
2 B. E. Kohler, *Chem. Rev.*, 1993, **93**, 41.
3 J. Saltiel, D.-H. Ko and S. A. Fleming, *J. Am. Chem. Soc.*, 1994, **116**, 4099.
4 (*a*) Y. Sonoda and Y. Suzuki, *J. Chem. Soc.*, *Perkin Trans. 2*, 1996, 401; (*b*) Y. Sonoda and Y. Suzuki, *Chem. Lett.*, 1996, 659; (*c*) Y. Sonoda, H. Morii, M. Sakuragi and Y. Suzuki, *Chem. Lett.*, 1998, 349; (*d*) Y. Sonoda, Y. Kawanishi and M. Sakuragi, *Chem. Lett.*, 1999, 587.
5 (*a*) P. J. Trotter and J. Storch, *Biochim. Biophys. Acta*, 1989, **982**, 131; (*b*) M. T. Allen, L. Miola and D. G. Whitten, *J. Am. Chem. Soc.*, 1988, **110**, 3198.
6 (*a*) D. R. Kanis, M. A. Ratner and T. J. Marks, *Chem. Rev.*, 1994, **94**, 195; (*b*) R. Cammi, B. Mennucci and J. Tomasi, *J. Am. Chem. Soc.*, 1998, **120**, 8834; (*c*) Y. Sonoda, Y. Suzuki, E. Van Keuren and H. Matsuda, *Macromolecules*, 1996, **29**, 288.
7 D. Döpp, *Top. Curr. Chem.*, 1975, **55**, 51.
8 (*a*) R. B. Cundall, I. Johnson, M. W. Jones, E. W. Thomas and I. H. Munro, *Chem. Phys. Lett.*, 1979, **64**, 39; (*b*) I. D. Johnson, E. W. Thomas and R. B. Cundall, *J. Chem. Soc.*, *Faraday Trans. 2*, 1985, **81**, 1303.
9 G. Pistolis and A. Malliaris, *Chem. Phys.*, 1998, **226**, 83.

10 W. H. Melhuish, *J. Phys. Chem.*, 1961, **65**, 229.
11 M. Towrie, A. W. Parker, W. Shaikh, P. Matousek, *Meas. Sci. Technol.*, 1998, **9**, 816.
12 P. Matousek, M. Towrie, A. Stanley and A. W. Parker, *Appl. Spectrosc.*, 1999, **53**, 1485.
13 S. K. Chattopadhyay, P. K. Das and G. L. Hug, *J. Am. Chem. Soc.*, 1982, **104**, 4507.
14 R. Bensasson, C. R. Goldschmidt, E. J. Land and T. G. Truscott, *Photochem. Photobiol.*, 1978, **28**, 277.
15 A. Harriman, *J. Chem. Soc.*, *Faraday Trans. 2*, 1981, **77**, 1281.
16 A. Harriman, G. Porter and M.-C. Richoux, *J. Chem. Soc.*, *Faraday Trans. 2*, 1981, **77**, 833.
17 C. W. Spangler, R. K. McCoy, A. A. Dembek, L. S. Sapochak and B. D. Gates, *J. Chem. Soc.*, *Perkin Trans. 1*, 1989, 151.
18 C. C. Leznoff and R. J. Hayward, *Can. J. Chem.*, 1972, **50**, 528.
19 S. L. Murov, I. Carmichael and G. L. Hug, *Handbook of Photochemistry*, 2nd edn., revised and expanded, Marcel Dekker Inc., New York, 1993, pp. 284–287.
20 J. Saltiel, D. F. Sears, Jr., Y.-P. Sun and J.-O. Choi, *J. Am. Chem. Soc.*, 1992, **114**, 3607.
21 P. C. Alford and T. F. Palmer, *J. Chem. Soc.*, *Faraday Trans. 2*, 1983, **79**, 433.
22 T. Itoh and B. E. Kohler, *J. Phys. Chem.*, 1987, **91**, 1760.
23 J. Saltiel and S. Wang, *J. Am. Chem. Soc.*, 1995, **117**, 10761.
24 For the charge transfer accompanied by single bond twisting see: (*a*) K. Bhattacharyya and M. Chowdhury, *Chem. Rev.*, 1993, **93**, 507; (*b*) W. Rettig, *Top. Curr. Chem.*, 1994, **169**, 254.
25 S. L. Murov, I. Carmichael and G. L. Hug, *Handbook of Photochemistry*, 2nd edn., revised and expanded, Marcel Dekker Inc., New York, 1993, pp. 345–348.
26 H. Görner, *Ber. Bunsenges. Phys. Chem.*, 1998, **102**, 726.
27 H. Görner, *Ber. Bunsenges. Phys. Chem.*, 1984, **88**, 1199.